Cellulose (2020) 27:4721–4743
https://doi.org/10.1007/s10570-020-03085-x

ORIGINAL RESEARCH

Correlation between the concentration and morphology of copper microparticles and their biocidal effect on paper sheets

P. Contreras · A. Amenabar · V. Apablaza · J. Martínez · R. Lavín · N. Silva

Received: 15 September 2019 / Accepted: 3 March 2020 / Published online: 9 March 2020

Abstract In this study, different methods for incorporating mixed or laminar copper microparticles (CuMPs) during papermaking were evaluated to determine the optimum paper-making process and correlate particle concentration and shape with antimicrobial activity. The addition of CuMPs during the disintegration of dry pulp stage was observed to produce a paper with uniformly distributed CuMPs, as determined through optical microscopy and UV–Vis spectroscopy analyses by measuring absorbance spectra in different areas of papers. Determination of two indices related to the concentration and distribution of copper will allow to predict the copper content in other papers. CuMP-paper samples were evaluated for structural, optical, and mechanical strength properties according to paper industry standards. Quantitative analyses by atomic absorption showed that between 24 and 39% of CuMPs were embedded in the paper fibre, independent of particle type. Finally, antibacterial activity analyses were performed according to ISO 20645 and ISO 20743. The results showed that papers with 0.30 g of incorporated CuMPs have antimicrobial activity, independent of particle morphology, with effects observed towards Gram (+) and Gram (−) bacteria and fungus. Furthermore, the evaluation of antimicrobial activity at different times of exposure to the microorganisms showed differences in effects that were dependent on the shape of the CuMPs incorporated into paper, where laminar particles exerted a sufficient effect, while no or a slight effect was observed for mixed CuMPs against *Aspergillus niger*.

Electronic supplementary material The online version of this article (https://doi.org/10.1007/s10570-020-03085-x) contains supplementary material, which is available to authorized users.

P. Contreras · A. Amenabar · N. Silva (✉)
Facultad de Diseño, Universidad del Desarrollo, Avenida Plaza 680, 7610658 Las Condes, Santiago, Chile
e-mail: nrsilva@udd.cl

V. Apablaza
Ciencia aplicada e ingeniería en Materiales y Geociencias SPA, Avenida Peñaflor Parcela 20, 9751379 Peñaflor, Santiago, Chile

J. Martínez
Centro de Medicina Regenerativa, Facultad de Medicina, Clínica Alemana-Universidad del Desarrollo, Avenida Las Condes 12,438, 7710162 Lo Barnechea, Santiago, Chile

R. Lavín (✉)
Facultad de Ingeniería y Ciencias, Universidad Diego Portales, Ejército 441, 8370191 Santiago, Chile
e-mail: roberto.lavin@udp.cl

R. Lavín
Centro Para el Desarrollo de la Nanociencia y Nanotecnología (CEDENNA), 9170124 Santiago, Chile

Graphic abstract

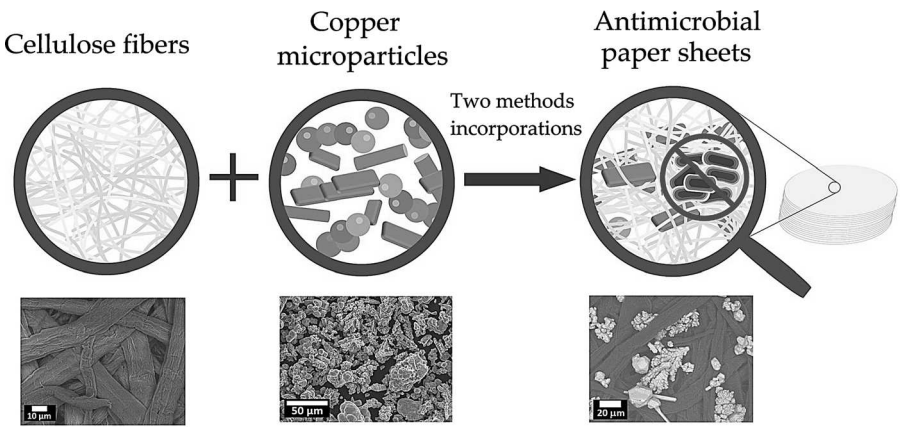

Keywords Paper · Paper-making · Cellulose · Copper · Antimicrobial · Biocide · Microparticles · Laminar · Nanoparticle · Characterization · Spectroscopy

Introduction

Paper is defined as a thin layer of plant fibres produced by drying a suspension of fibres in water, where cellulose and, to a lesser extent, starch are the primary components (Maurer 2009). Depending on their use, paper can be classified into four groups, drawing, wrapping, hygienic, and specialty papers, the latter of which includes filter, decorative, and self-adhesive paper, among others. The raw material, weight, finish, structure, and nature of the surface will determine the properties of a particular type of paper (Holik 2006).

In recent years, paper has become attractive as a base material for various applications, either by modifying its structure or mixing it with other materials to achieve different or enhanced properties according to specific requirements. For example, paper has been studied as a support for energy harvesting devices in paper-based fuel cells (PBFCs), passively transporting aqueous electrolytes by capillarity. PBFCs have been tested for various fuels, including methanol (Esquivel et al. 2014), glucose (Dector et al. 2017), hydrogen peroxide (Mousavi Ehteshami et al. 2016), and even H_2 (Esquivel et al. 2017). There is a growing interest in producing paper-based detection platforms due to the porous and high surface-to-volume ratio the cellulose substrate offers, allowing for small devices to be generated and reducing analysis times (Wang et al. 2012). Furthermore, because paper is an economical material, there are many benefits associated with its widespread use and acceptance in the world market for various applications, such as in temperature and humidity sensors (Mahadeva et al. 2011), fluorescence immunoassays (Liang et al. 2012), and chemiluminescence (Wang et al. 2012), among others (Kim et al. 2010; Jokerst et al. 2012; Nery and Kubota 2013; Chen et al. 2016; Esquivel et al. 2017). Another field of interest is related to the use of paper in separation and purification systems and as filter paper, where it is studied/applied for a variety of purposes, such as in the collection and analysis of blood samples (Mei et al. 2001), electrophoresis (Kunkel 1951) and the determination of soil moisture (Fawcett and Collis-George 1967), among others (Chardon et al. 1996). For many applications, it is essential to modify the paper surface such that it can last over time, since its constituent hydrophilic polysaccharides can serve as nutrients for microorganisms (Koziróg et al. 2019). Therefore, a great deal of effort has been made to obtain paper surfaces with antifungal and antibacterial properties (Sequeira et al. 2012). To this end, various agents have been incorporated into the structure of paper, such as cationic surfactants hexamethylene-1,6-bis-(*N*,*N*-dimethyl-*N*-dodecyl ammonium bromide) (C6) and its monomeric analogue didecyldimethyl ammonium chloride (DDAC) mixed with starch or applied in aqueous solution by spraying, which was shown to effectively protect paper from *Aspergillus*

brasiliensis, *Aspergillus terreus*, *Penicillium chrysogenum*, *Penicillium aurantiogriseum*, *Trichoderma viride*, *Chaetomium globosum*, *Bacillus subtilis* and *Pseudomonas aeruginosa* (Koziróg et al. 2019). In addition, the treatment of paper with chitosan dissolved in lactic acid has been shown to increase its brightness and act as an oxygen barrier, showing antibacterial effects against *B. subtilis* (Vartiainen et al. 2004). Furthermore, chitosan and quaternary ammonium salts provide good bacterial inhibition and resistance to paper, although they have poor antifungal effects (Nechita et al. 2015). Paper coated with a ternary carbohydrate mixture (alginate, carboxymethyl cellulose, and carrageenan) and grapefruit seed extract showed strong antibacterial activity against food-borne pathogenic bacteria, such as *Listeria monocytogenes* and *Escherichia coli*, which were destroyed after 3 and 9 h, respectively (Shankar and Rhim 2018). Filter papers embedded with copper sulfate and copper oxides are also active antibacterial agents against *E. coli* and *Staphylococcus aureus*, showing severe and moderate effects, respectively. The reactivity of these filter papers against two fungal species, *Candida albicans* and *Aspergillus niger*, has been studied using disc diffusion method with modest effects, producing relatively small inhibition zones (Cano et al. 2018). Particular attention has been given to metal nanoparticles due to their greater activity compared with organic antimicrobial agents or metal ions, with outstanding activity observed for silver nanoparticles (AgNPs) (Dankovich and Gray 2011; Imani et al. 2011; Ghorbani 2014; Amini et al. 2016; Dankovich et al. 2016; Xu et al. 2018; Zhai et al. 2018), Ag-Au core-shells (Tsai et al. 2017), TiO_2 nanobelt-silver nanoparticles (Wang et al. 2013), silver oxides (Jain et al. 2018), zinc oxides (Martins et al. 2013; Pang et al. 2016; Jain et al. 2018), and copper sulfide (Huang et al. 2017). In particular, copper nanoparticles (CuNPs) incorporated into paper have been intensively studied for their strong antibacterial activity against a large variety of microorganisms as well as their lower cost compared to AgNPs (Dankovich and Smith 2014). Various techniques have been used to prepare CuNP-paper composites through in situ and ex situ preparation routes (Tamayo et al. 2016). From in situ preparation methods, CuNP papers have been obtained from cotton dissolved in a solution of cuprammonium hydroxide that is subsequently poured into a glass and coagulates to obtain paper sheets. Copper-paper sheets show efficient antibacterial activity against *S. aureus* and *E. coli*, with a decrease in bacterial viability observed after 0.5 h of exposure and complete bacterial eradication after 1 h (Jia et al. 2012). CuNP papers have also been obtained from sheets that were immersed in a copper hydroxide solution and subsequently reduced by ascorbic acid. These papers have been evaluated as filters for water purification by filtering *E. coli* suspensions through them. CuNP-paper sheets inactivate bacteria that pass through them, and the copper levels released into the effluent water remain below the recommended drinking water limit (1 ppm) (Dankovich and Smith 2014). The same sheets of filter paper have been tested using real water samples from contaminated streams. In less polluted streams (250–15,000 CFU/100 mL), AgNPs and CuNPs completely inactivate coliform bacteria, whereas in waters with higher levels of these bacteria (500,000–1,000,000 CFU/100 mL), with reductions of log10 5.1 for AgNPs and log10 4.8 for CuNPs. The results obtained using *E. coli* followed similar trends (Dankovich et al. 2016). Copper oxide nanoparticles (CuONPs) prepared ex situ have also been studied for the same water purification purposes, showing antibacterial effects against *E. coli*, *B. subtilis*, *P. aeruginosa*, and *Bacillus cereus* (Jain et al. 2018). Another ex situ report describes the generation of Kraft paper coated with CuNP-chitosan by dipping and its superior antimicrobial activity against *E. coli* compared to *B. subtilis* (Ghorbani 2017). However, to date, few similar studies have been performed using copper microparticles (CuMPs) or their respective oxides (CuOMPs). Emam et al. show the in situ preparation of CuOMPs on cellulose fibres obtaining a 90% reduction of bacterial viability against *S. aureus* after three hours of contact time (Emam et al. 2014). Szekeres et al. show the use of spherical CuMPs 1–5 μm indiameter coating cellulose-based water filters for MS2 bacteriophages retention achieving a virus retention at least 5 magnitudes at three different pH values (Szekeres et al. 2018).

It should be noted that because the type of copper (ionic or particulate), its oxidation state, size, and shape are characteristics that determine the mechanism of antibacterial action, the appropriate selection of material, based on the specific application, is crucial. Because of their size, CuNPs can bind strongly to or become internalised by cells, causing oxidative

stress and severe damage to DNA in vitro, making CuNPs more toxic than their micro-analogues (Kaweeteerawat et al. 2015). The antimicrobial properties of papers with biocidal particles is controlled by their distribution, aggregation, and concentration on the paper surface. Therefore, the method used to incorporate copper particles into paper sheets during the manufacturing process is crucial to ensure homogeneous distribution. Furthermore, it is important to characterise and determine the concentration, distribution, and aggregation state of the biocidal particles (Ngo et al. 2011).

Considering the above information, the present study describes the preparation of paper sheets by incorporating CuMPs at three different concentrations to assess their potential use in future applications with the benefit of having decreased genotoxicity in cells compared with CuNPs. Importantly, the antimicrobial effect of copper is clearly associated with contact, i.e., a good distribution of CuMPs between the cellulose fibres is necessary such that the paper surface does not allow the proliferation of microorganisms. This study reports the incorporation of CuMPs into paper by an in situ route for paper manufacturing, whereas the microparticles were obtained ex situ. Two methods were used for incorporating the particles (during the first stage of pulp disintegration and the second stage of paper sheet-forming) to determine the optimal conditions for incorporating CuMPs to produce paper sheets with evenly distributed particles. Finally, the results obtained through various characterisation techniques were correlated with those of various microbiological tests to predict the efficacy of the biocidal surface under other working conditions.

Materials and methods

Four types of CuMPs were used in this study (see Table 1). The samples were delivered by *Química y Minera Puebla SPA* (Santiago, Chile) and used as received.

Characterisation of the sheet of white paper and copper particles

The starting materials were first characterised using a scanning electron microscope (SEM) JEOL JSM-6010LA equipped with a large field low vacuum detector to determine the distribution of cellulose fibres in the white paper and the morphology of the commercial copper particles, image analysis was performed for a population of 100 particles, using ImageJ. The CuMP size distribution was determined through laser diffraction analysis (LDA) using a Malvern Panalytical Mastersizer 2000.

Paper production and incorporation of copper microparticles

The experimental method used to develop antimicrobial paper is based on standard paper manufacturing procedures according to ISO 5269-1:2005. The stages described below correspond to the process used to prepare circular sheets obtained from a pulp suspension.

1. Disintegration of dry pulp: 30 g of dried pulp is disintegrated in 2 L of demineralised water at 30,000 revolutions.
2. Dilution and homogenisation: The sample is diluted with demineralised water to reach a volume of 10 L, or a 0.30% concentration, and homogenised using an industrial-grade Waring blender at 15,000 rpm for 5 min.

Table 1 Physical parameters of copper particles delivered by the supplier

Particle type	Geometry	Purity (%)	Tyler mesh size (Tyler)	Average equivalent diameter (μm)
T1	Mixed	99.50	< 450	< 30
T2	Mixed	99.50	< 850	< 15
T3	Laminar	99.88	< 450	< 30
T4	Laminar	99.88	< 850	< 15

Particle type, geometry, purity, and size

3. Drainability measurement: performed within the first hour after the homogenisation process (ISO 5267-1:1999).
4. Pulp suspension consistency measurement: The consistency of the pulp suspension in the sheet former is measured.
5. Volume determination: The volume of the sheets corresponding to 1.21 g of dried pulp is determined.
6. Sheet forming: a conventional Labtech (Semi-Automatic) Sheet Former machine, Model 300-0 is used to obtain a 16 cm diameter paper sheet. Next, the sheet of paper is placed between Ederol filters to extract excess water. Then, the sheet is pressed for 5 min at 410 ± 10 kPa, which is repeated on the back of the sheet for 2 min at the same pressure.
7. Drying and calendering: The test sheets are dried at a temperature of 94 ± 3 °C for approximately 8 min. Finally, the sheets are pressed in a heated room at 23 ± 1 °C with 50 ± 2% relative humidity for at least 3 h before performing physical and mechanical measurements.

Paper containing copper particles was produced following two methods for incorporating the particles, which consisted of adding the copper particles either during disintegration of dry pulp or sheet-forming stages (stages 1 and 6, respectively).

Method 1 Preparation of CuMP-paper, incorporating the particles during the disintegration stage (1). Three different masses of CuMPs (0.05, 0.10, and 0.30 g) were mixed per 1.21 g of cellulose until 15 g of cellulose was obtained to manufacture 10 paper sheets for each presentation. The cellulose-copper mixture was homogenised in a disintegrator with 2 L of water at 30,000 rpm. Then, the sample was homogenised in 5 L of demineralised water for 5 min, and then the process was continued.

Method 2 Preparation of CuMP-paper, incorporating the particles during the sheet-forming stage (6). The standard cellulose-water mixture was deposited into the sheet former, after which the CuMPs were immediately added at three different amounts (0.05, 0.10, and 0.30 g) per 1.21 g of cellulose. The sheet former used approximately 5 L of water that was stirred for 5 s, after which the water was drained by gravity to form the paper.

Characterisation of CuMP-paper

The copper distribution in the cellulose fibres was determined by UV–Vis spectroscopy using a Shimadzu UV 1280 spectrophotometer. In addition, the papers were characterised using a Leica DM4000 microscope for material analysis under bright- and dark-field illumination. The distribution of copper particles between cellulose fibres was assessed using an Olympus IX81 microscope using wide-field fluorescence, and a histogram of the results was generated. Image analysis was performed using ImageJ, and the morphological analysis used to discriminate particles included using a combination of dilatation and erosion filters of the images. The particles were evaluated over an area of 10 μm^2, equivalent to an average radius of 1.94 μm, since morphological filtering discards particles of smaller sizes due to variations in image intensity. The average particle radius was obtained assuming a circumference of area A such that the average radius will be $r = \sqrt{A\pi^{-1}}$. In addition, the samples were characterised using JEOL JSM-6010LA SEM equipped with a large field low vacuum detector.

The copper content embedded in the paper sheets was determined by atomic absorption analysis using a PerkinElmer AAnalyst^{TM} 700 high-performance atomic absorption spectrometer. X-ray diffraction analysis was performed to identify the type of copper in the particles using a Bruker D8 Advance, Kα1 Cu (λ = 1.5406 nm).

A Bruker Vertex 80v infrared spectrophotometer was used to perform Fourier transform infrared spectroscopy (FTIR) at a resolution of 0.2 cm^{-1} to identify changes in the cellulose spectrum, which were attributed to possible Cu-paper interactions.

The physical and mechanical properties of the paper sheets were determined using the following equipment under the respective ISO standards. To determine weight, the ISO 536:1997 standard was followed; thickness was determined using a Lorentzen & Wettre (L & W) micrometer (ISO 534:2005); tensile strength was assessed using an L&W tensile tester SE 062/SE 064 (ISO 1924-3:2005); tearing resistance was evaluated using an L&W tearing tester 009 (ISO 1974:2012); and bursting strength was assessed using an L&W Bursting Strength Tester SE 180/SE 181 (ISO 2758:2014). To evaluate the porous structure of the paper, Gurley porosity was determined using an

L&W air permeance tester, SE 166 (ISO 5636-5:2003); and optical properties were evaluated in an L&W Elrepho® to assess whiteness (ISO 2470-1:2016), opacity (ISO 2471-98), yellowness, and colour (ISO 5631-1:2009).

Antimicrobial analysis

Sample preparation From a 16-cm diameter sheet of paper, 2.54 cm circular samples were obtained using a punch. The samples were handled with gloves after their manufacture and stored individually at room temperature, protected from light.

Antimicrobial activity was evaluated according to ISO 20645:2004 (Textile fabrics-Determination of antibacterial activity-Agar diffusion plate test). This method pertains to the determination of the antibacterial effect of treatments applied to textile fabrics. The method states that it can be used to test other materials, properly adapted Therefore, because many textiles are composed of a high percentage of cellulose, the applicability of the method to paper samples is acceptable.

Twelve samples (No. 2-13, identified in Table 3) containing the four assayed types of CuMPs with different copper contents (0.05, 0.10, and 0.30 g) were preliminary evaluated against *S. aureus* ATCC® 29213™ and *Klebsiella pneumoniae* ATCC® 700603™ to determine the samples that have antimicrobial activity and thus delimit the expanded work to five strains using two methods of analysis.

Bacteria growth: from a pure culture of each microorganism, a subculture was carried out in liquid LB medium at 37 °C for 18 h, with constant agitation at 160 rpm. From this fresh culture inoculums were prepared containing 10^6 CFU/mL for bacterial growth in the upper agar layer. Samples were placed on two-layer agar plates. The lower layer consisted of Luria-Bertani Broth agar (Difco) without bacteria (10 mL), and the upper layer consisted of the same agar culture medium (5 mL) that had been previously inoculated with the selected bacterial strain (10^6 CFU/mL) prior to gelling. Plates were incubated at 37 °C for 24 h immediately after placing the paper sample on the agar. Antibacterial activity was evaluated according to the extent of bacterial growth in the contact area between the agar and the paper, and paper without copper was used as a control (Sample No. 1). In those samples showing antimicrobial activity, the inhibition zones around the paper circles were measured using a digital caliper. To digitize the inhibition zones, the Petri dishes were imaged at a resolution of 300 dpi (in photo mode, colour) using a Lexmark X656 scanner from Lexmark International Inc.

At the end of the test, the bacterial colonies of both strains were stained with 0.1% Coomassie blue R-250 (Coomassie® Brilliant blue R 250 Merck) dissolved in water:methanol:acetic acid (4:5:1) to better observe the contrast and categorise their apparent density and size. Micrographs were taken on a Carl Zeiss Stemi 2000-C stereo microscope with an AxioCam ERc 5 s Rev. 2.0 microscopy camera and analysed using AxioVision (v 4.8.2.0, Carl Zeiss MicroImaging GmbH). Antibacterial activity was calculated according to ISO 20645:2004 as detailed in "Appendix".

Subsequently, the samples with the highest copper content (No. 4, 7, 10, and 13) were evaluated for antimicrobial activity, qualitatively (according to ISO 20645:2004, previously described) and quantitatively (according to ISO 20743:2007), against other bacteria and fungi. The culture media used for the assayed strains are as follows: *S. aureus* ATCC® 6538™/Trypticase Soy Agar/1% Potassium Tellurite (Merck); *E. coli* ATCC® 25922™/Trypticase Soy Agar (Merck); *A. niger* ATCC® 16404™/potato dextrose agar (Merck); *C. albicans* ATCC® 90028™/potato dextrose agar; and *Penicillium* sp. ATCC® 11597™/potato dextrose agar. The test agar plates were incubated at 37 °C for 24 h, while fungi were incubated at 30 °C for up to 96 h. Subsequently, inhibition zones were observed around the paper samples. "Appendix" details the calculations and determinations of antibacterial activity effects, which were performed according to ISO 20645.

Quantitative assessment was performed using 4 × 4-cm paper samples by exposing them to a standard inoculum (10^6 CFU/mL or 10^5 conidia/mL) of the target strain and determining the number of viable colonies at two stages: 0 and 24 h of incubation at 37 °C. The results are expressed as the average count of viable colonies that grew on the post-incubation plates. "Appendix" details the calculations and determinations of antibacterial activity effects, which were performed according to ISO 20743:2007.

Finally, using the absorption method described in ISO 20743:2007, the minimum exposure times required to observe the antimicrobial effects of samples 4 and 10 against *S. aureus* ATCC 6538,

E. coli ATCC 25922, and *A. niger* ATCC 16404 were determined using the culture media described above. The samples were exposed to a standard inoculum (10^6 CFU/mL) of the target strain at 0, 0.5, 1, 2, and 3 h. The number of viable colonies was assessed by duplicate plate count, and the results are expressed as the number of viable colonies that grew on the plates at different times post-incubation.

Results

Characterisation of the sheet of white paper and copper particles

The white paper sheet sample was characterised by SEM. Figure 1 shows the micrograph of the sheet of white paper, where nonwoven cellulose fibres with diameters between 7 and 22 μm can be observed (the spaces or voids between the fibres are called vessels). Vessels can incorporate impurities (coal or other), and depending on the amount incorporated can become visible to the naked eye. A macroscopic representation of these vessels can be determined according to ISO 5350, "Estimation of dirt and shives", where the presence of coal or paint is evaluated by backlight using a comparison template. For this reason, the observed vessels were determined to provide an appropriate space to incorporate copper particles.

CuMPs were characterised by SEM to determine their shape and size. Figure 2a, b show the T1 and T2 particles corresponding to mixed particles with quasi-spherical, dendritic, cubic, and amorphous shapes. The histogram exhibits size of 10.20 ± 8.673 μm and 9.979 ± 10.69 μm for a population of 100 particles (the widest side of each particle was considered) and no differences in size were observed between both samples due to particle heterogeneity.

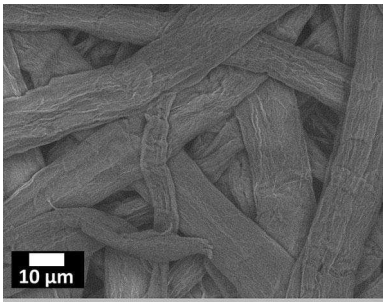

Fig. 1 SEM micrograph of cellulose fibres on the sheet of white paper

In contrast, the SEM images of laminar microparticles presented in Fig. 2c, d show the predominant presence of structures with that shape, and no significant differences in particle size were observed in these samples, 11.66 ± 13.90 μm and 11.42 ± 12.45 μm for T3 and T4, respectively.

The CuMP size distribution was determined through Laser Diffraction Analysis (LDA). Through this technique, it is possible to show the difference in size between the sample T1 and T2, where 50% of the population has sizes of 22,952 μm and 14,600 μm, respectively. Values obtained were similar to those reported by the supplier of < 30 μm and < 15 μm.

Production and characterisation of CuMP-paper

Figure 3 shows optical micrographs and dark-field images of white paper without CuMP (Fig. 3a, d) and those with 0.30 g of mixed T1 copper particles obtained following the two previously mentioned methods used for their incorporation. Figure 3b shows paper generated by incorporating CuMPs during the disintegration of dry pulp stage. An evenly coloured paper can be observed due to copper particles having been in contact with cellulose fibres during the first step of papermaking, resulting in a better dispersion and distribution of CuMPs among the fibres during sheet formation. The same results can be observed in the dark-field micrograph (Fig. 3e), where particles of different sizes are observed among the fibres distributed throughout the surface, the CuMPs are easily observed due to their reflecting light with a bright coppery colour. The results shown in Fig. 3c are different, as the paper has an irregular colour with dark brown spots and holes, indicative of a poor distribution of copper particles in the cellulose fibres. The second method for incorporating copper particles at a more advanced stage in the process used to make paper sheets was developed to minimise the loss of copper during the various steps of paper production. However, since the cellulose-CuMP mixing process lasted only 5 s, most of the copper particles preferably agglomerated on the water surface due to their hydrophobic nature. Finally, when water decantation occurs, paper sheets with isolated copper particles and clusters that are primarily distributed on the surface are obtained, causing perforations in the sheet after

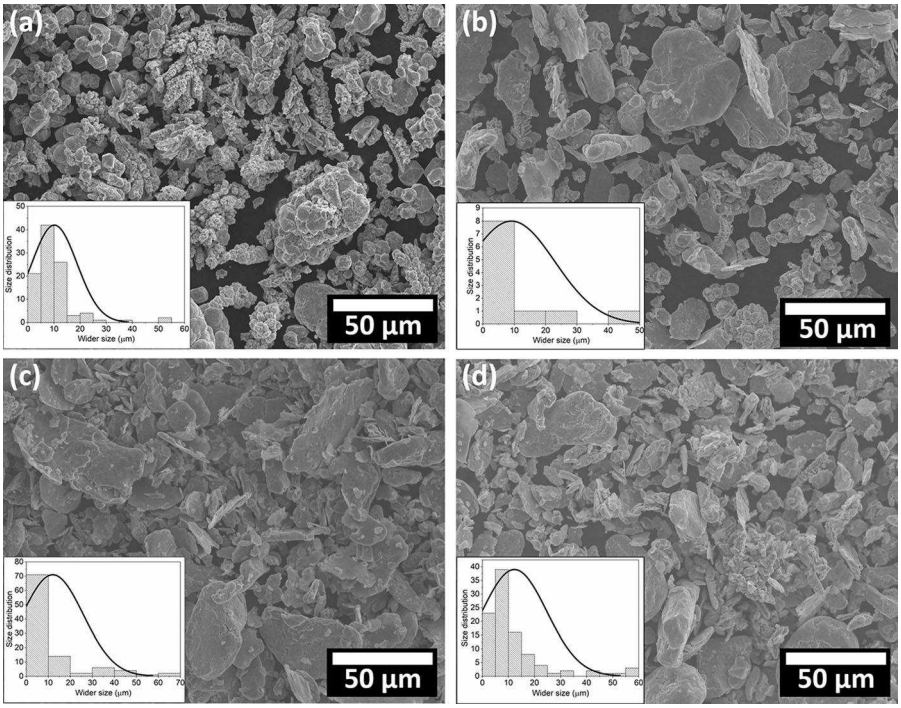

Fig. 2 SEM micrographs of the different types of microparticles. Mixed **a** T1 (diameter 30 < µm), **b** T2 (15 < µm). Laminar **c** T3 (30 < µm), **d** T4 (15 < µm), with their respective particle size distribution histograms

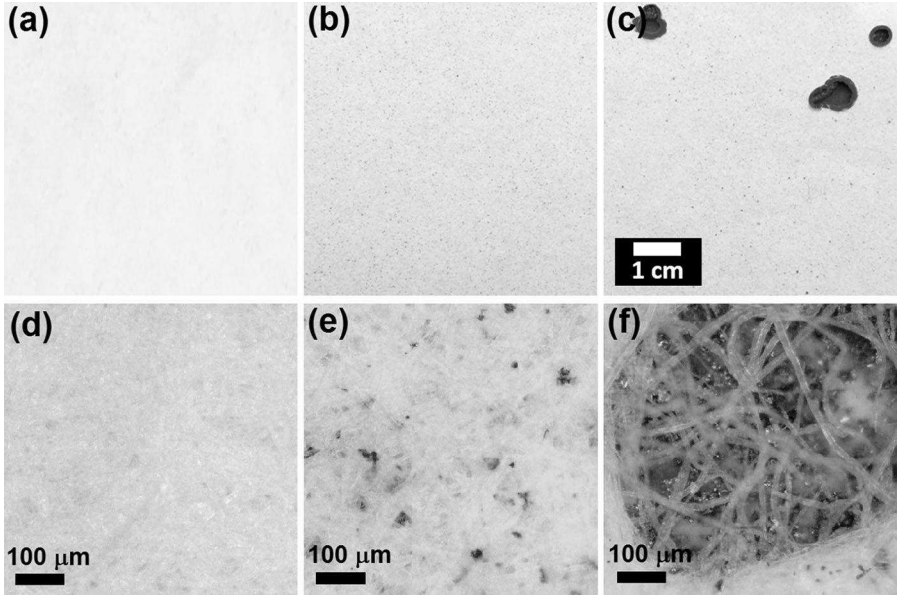

Fig. 3 Images of the paper: **a** control without CuMP, and papers with 0.30 g of T1 CuMP following the incorporation methods **b** 1 and **c** 2 and their corresponding dark-field optical micrographs (**d**, **e**, and **f**)

water drainage. Figure 3f shows a coppery CuMP cluster among isolated cellulose fibres, weakening the paper surface and leaving it susceptible to future damage.

To determine the distribution of CuMPs on the paper surface, spectrophotometric analyses of the three papers shown in Fig. 3 were performed. Figure 4 shows the absorption spectrum of the white paper control (T1 C = 0.00 g), where three UV absorption peaks at 265, 300, and 350 are observed that can be attributed to $n \rightarrow \pi*$ and $\pi \rightarrow \pi*$ transitions of conjugated ketones and enol groups, provided by carbonyls derived from the ageing of cellulose (Łojewska et al. 2007). In addition, the UV–Vis spectra of the papers with 0.30 g of incorporated CuMPs are shown for both tested methods. The spectra contained additional peaks compared to those observed in the control paper due to the presence of Cu. Some studies have reported that materials with sizes smaller than the wavelength of electromagnetic radiation have an absorption band that is associated with the phenomenon of surface plasmon resonance. In this study, although we used T1 CuMP,—which should preferably have sizes of less than 30 µm (Table 2)—the peak at 450 nm is consistent with copper oxide nanoparticles (Silva et al. 2019). This result was confirmed by the dark-field optical micrograph shown in Fig. S1, where microparticles are observed in the paper vessels as well as the cellulose fibres. An absorption band at 450 nm was also observed in the absorption spectra of papers with 0.30 g of T2, T3, and T4 CuMPs. The absorption spectra of papers with 0.30 g of T1 CuMPs incorporated via method 2 only show a slight increase in absorbance compared with the control, but without the peak at 450 nm.

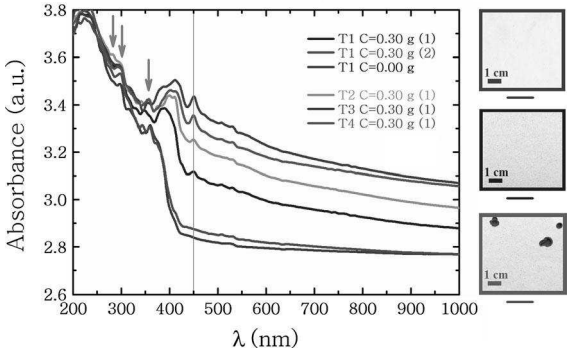

Fig. 4 UV–Vis absorbance spectra of the control paper without CuMP and after 0.30 g of T1 CuMPs were incorporated following methods 1 and 2, and of papers with 0.30 g of T2, T3, and T4 CuMPs incorporated following method 1

Table 2 Particles size distribution, values of the specific area and expressed in percentile

Type	Specific area (m^2/g)	D_{10} (µm)	D_{50} (µm)	D_{90} (µm)
T1	0.0358	9.626	22.952	43.780
T2	0.0531	6.819	14.600	27.183
T3	0.0447	7.069	19.765	41.388
T4	0.0611	5.365	13.480	28.034

To perform a statistical analysis of the concentration and distribution of particles in different areas of the papers shown in Fig. 4, two indices determined from the UV–Vis spectroscopy curves were defined: one related to the absorbance amplitude at 450 nm (I_λ) and the other to the area under the curve between 200 and 1000 nm (I_a). Figure 5 shows the graphs of the amplitude and area indices associated with different areas of the paper. The black dots correspond to the absorbance amplitude at 450 nm and the blue dots to the area under the spectrum (Fig. S2 shows the absorption spectra for each area). These indices represent the particle concentration in the paper, and when plotted according to the different areas of the paper, they represent the dispersion or homogeneity of copper distribution in the sample. Figure 5a shows that the four areas of the paper produce indices with similar

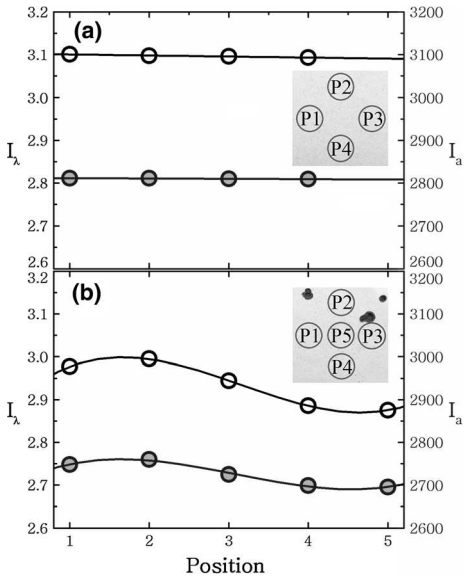

Fig. 5 Graphs of the indices of absorbance amplitude at 450 nm and the area under the curve in different areas of the paper with T1 CuMPs incorporated following methods **a** 1 and **b** 2

values (3.1 and 2800 for amplitude and area indices, respectively), confirming the homogeneous distribution of copper particles in the paper. In contrast, Fig. 5b shows indices with different values in the five areas analysed, presenting indices with values lower than those obtained in Fig. 5a Thus, much of the incorporated copper may have been dragged into the water through the perforations during draining, resulting in copper being concentrated at the edges of the holes or in specific aggregates (as shown in Fig. 3c) such that their concentration could not be determined using this method (because of the masking effect of particles in the aggregates).

Since the first method for incorporating CuMPs (during the disintegration of dry pulp stage) was shown to produce paper sheets with evenly distributed copper particles, all subsequent tests were performed using this method.

Subsequently, the number of CuMPs incorporated was changed, decreasing to 0.10 or 0.05 g to obtain trends in the indices associated with the paper copper concentration. Figure 6 shows images of CuMP-paper made with different types (T1, T2, T3, and T4) and concentrations of CuMPs. A higher amount of copper results in a darker paper, which differs in colour intensity depending on whether mixed or laminar particles are used, with laminar particles resulting in a darker hue. In addition, UV–Vis spectra of the papers modified with the different types and concentrations of CuMPs were obtained. As an example, Fig. 7 shows

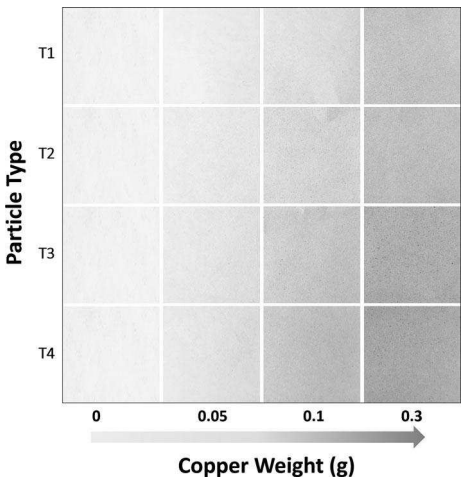

Fig. 6 Images of papers containing different types (T1, T2, T3, and T4) and amounts (0.00, 0.05, 0.10, and 0.30 g) of copper particles

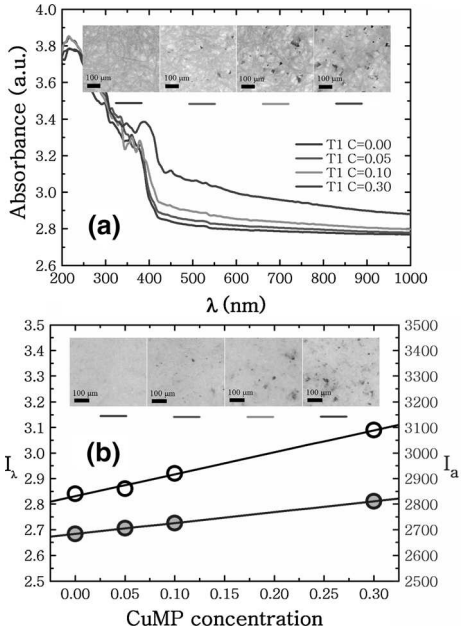

Fig. 7 **a** UV–Vis absorption spectra of papers with 0.00, 0.05, 0.10, and 0.03 g of T1 CuMPs with inset bright-field micrographs (transmission). **b** Plot of the amplitude and area indices versus CuMP concentration with inset dark-field micrographs (reflection)

the UV–Vis absorption spectra of the papers with 0.00, 0.05, 0.10, and 0.30 g of T1 CuMPs incorporated as well as their corresponding indices of absorbance amplitude at 450 nm and area under the curve. Furthermore, bright-field micrographs (transmission) and dark-field micrographs (reflection) presented in Fig. S3, show the papers made with different types and concentrations of CuMPs. Increasing the copper concentration produces an increase in absorbance throughout the spectral range, primarily due to the greater absorbance of microparticles and an increase in the peak intensity at 450 nm, resulting in a linear correlation between the amount of copper incorporated and the amplitude and area indices (Fig. 7b). This finding allows for copper absorption and the indices associated with other amounts of incorporated copper to be predicted. Bright-field micrographs allow for clear observations of cellulose fibres and copper particles, the latter of which appear as black spots, unlike dark-field micrographs, which show better-defined copper particles and the plane in which they are incorporated among the fibres when observed in reflection mode. In both cases, it is possible to confirm the linear trend between the number of CuMPs

incorporated into the fibres and the number of particles adsorbed on the paper.

Copper distribution analyses were performed in which wide-field fluorescence was measured to estimate the distribution and sizes of the microparticles incorporated into the cellulose fibres. This technique takes advantage of the autofluorescence of the sample, composed of vegetable fibres with high cellulose content, which can be observed in the brighter grey tones shown in Fig. S4 obtained from the white paper sample without copper particles. Figure 8 shows optical micrographs, obtained using a 4 × magnification objective, of the samples of CuMP-paper samples made with different types of CuMPs. Irregular particles of different sizes can be seen dispersed in the fibres. Each micrograph shows the corresponding size distribution chart, and Table 3 shows a summary of the information obtained. As the copper concentration increased, the percentage area occupied by copper particles proportionally increased. In addition, the average radii ranged from 6.314 to 7.404 μm for the mixed particles (T1 and T2) and from 6.247 to 7.683 μm for the laminar particles (T3 and T4), with no significant differences observed between different-sized particles of the same type. For example, when comparing the radii of the samples made with 0.30 g of T1 and T2 CuMPs (samples 4 and 7), no significant differences were observed in the average radii A potential explanation for this observation could be that incorporating copper particles at the initial stage of

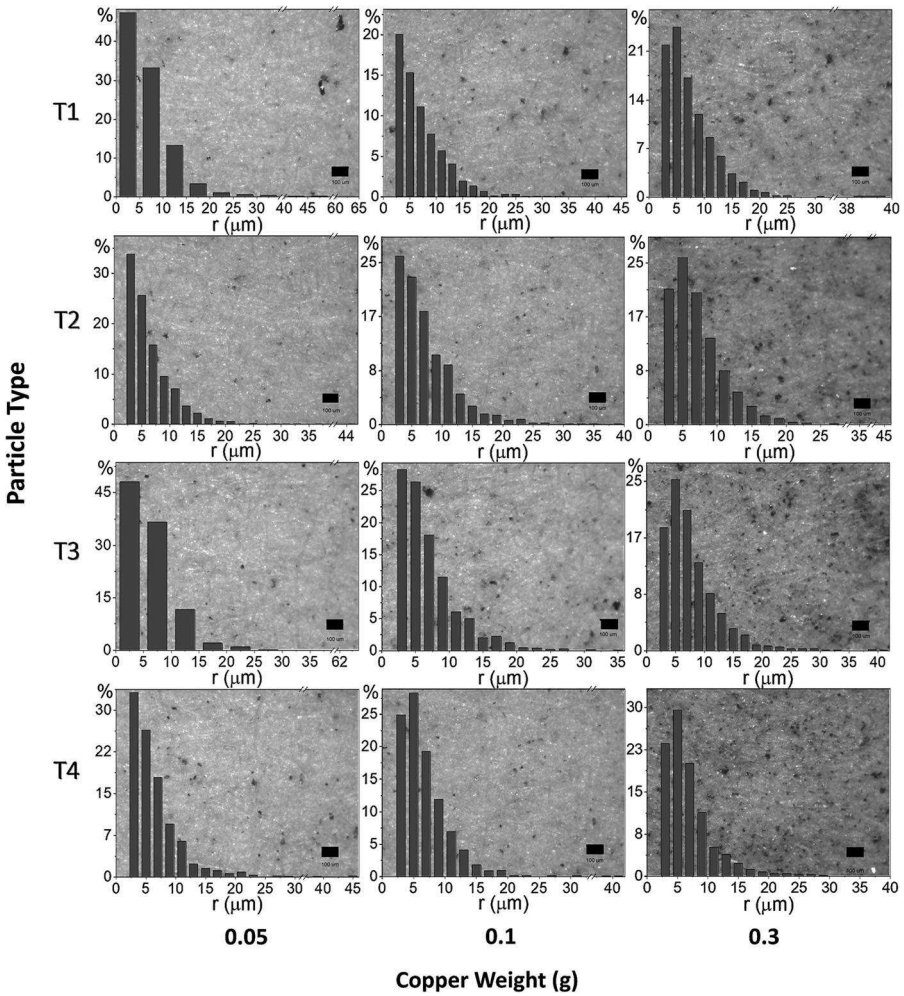

Fig. 8 Wide-field fluorescence micrographs of paper with different types (T1, T2, T3, and T4) and amounts (0.05, 0.10, and 0.30 g) of incorporated CuMPs and their corresponding histograms showing the CuMP size distribution. The bar equals 100 μm

Table 3 Numerical identification of the sample according to the type and weight of CuMPs incorporated

Sample	Type	Weight (g)	Micrographs (No.)	CuMPs (No.)	r [Min–Max] (μm)	< r > (μm)	SD (μm)	Area (%)
1	–	0.00	–	–	–	–	–	–
2	T1	0.05	20	1193	2.169–62.591	6.693	4.221	1.812
3	T1	0.10	16	1105	2.169–42.625	7.139	4.264	2.011
4	T1	0.30	18	1537	2.169–38.558	7.404	4.297	2.530
5	T2	0.05	21	1607	2.169–44.612	6.314	4.774	1.754
6	T2	0.10	21	1365	2.169–39.364	7.254	4.319	1.959
7	T2	0.30	22	2057	2.169–45.661	7.120	4.066	2.499
8	T3	0.05	22	1862	2.169–64.440	6.247	3.739	1.965
9	T3	0.10	19	1529	2.169–34.904	6.860	4.057	2.149
10	T3	0.30	19	1438	2.169–41.151	7.683	4.514	2.493
11	T4	0.05	17	1341	2.169–44.468	6.258	3.794	1.834
12	T4	0.10	17	1396	2.169–41.639	6.642	3.854	1.980
13	T4	0.30	20	1793	2.169–37.898	6.810	4.006	2.324

Number of micrographs analyzed by sample (micrographs), total number of CuMPs detected by sample (CuMPs), minimum and maximum radii of CuMP measured (r [Min–Max]), average radius of CuMPs (<r>), standard deviation (SD), and percentage of area occupied by the CuMPs per micrography (Area)

paper formation results in good particle dispersion in the sheet as well as with particle disaggregation.

SEM micrographs were also taken to assess the CuMP distribution and morphology of the CuMP-papers in more detail. Figure 9 shows SEM micrographs of the paper sheets with different amounts of T1 CuMPs. Embedded particles are seen on the paper surface and interstitially in the vessels of the cellulose matrix, where the higher the concentration of copper incorporated, the greater the number of particles embedded in cellulose fibres. This result agrees with previous analyses using UV–Vis spectroscopy and through optical micrograph observations. Figure 10 shows SEM micrographs of cellulose paper with 0.30 g of T1 and T3 CuMPs under different magnification. T1 particles can be seen to be incorporated in the fibre vessels and oriented in all directions due to their various shapes, facilitating the penetration of the material among the fibres (Fig. 10a), while Fig. 10b showing cellulose fibres with incorporated T3 particles. Laminar copper particles interact parallel to the surface of the sheet, with less material penetration into the fibres occurring. Therefore, since the morphology of CuMPs determines their dispersion among the cellulose fibres, it is possible to evaluate the different colour intensities acquired by papers according to the incorporated particle type, as seen in Fig. 6.

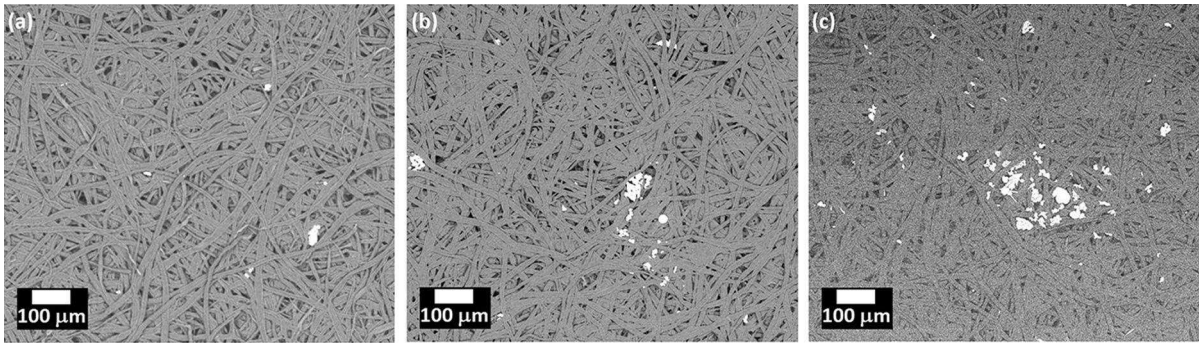

Fig. 9 SEM micrograph of cellulose paper with different amounts of T1 CuMP: **a** 0.05 g, **b** 0.10 g, and **c** 0.30 g

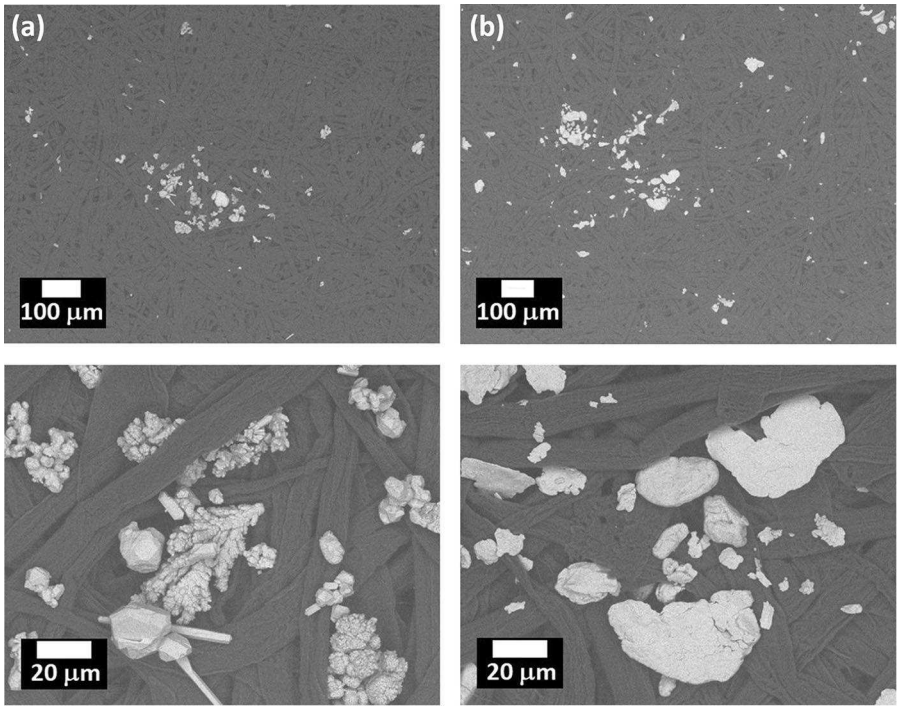

Fig. 10 SEM micrographs (at different magnifications) of cellulose paper with 0.30 g of **a** T1 (Sample No. 4) and **b** T3 (Sample No. 10) CuMPs

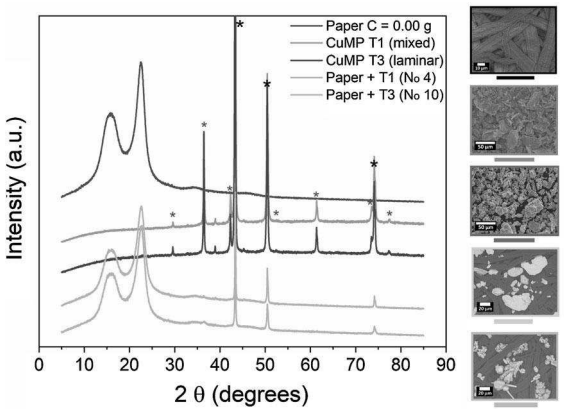

Fig. 11 X-ray powder diffraction patterns of cellulose paper, T1 and T3 CuMPs, paper with T1 and T3 CuMPs (Sample Nos. 4 and 10, respectively). SEM micrographs associated with each diffractograms

For comparative purposes, Fig. 11 shows the diffraction patterns that are obtained for paper cellulose sheets: type T1 (mixed) and type 3 (laminar) CuMPs; and papers with the corresponding CuMPs. The diffraction pattern obtained for the paper cellulose exhibited two mean peaks at 2θ value of 15.69° and 22.63° associated with cellulose type I (Gong et al. 2017). The same peaks appear in paper with CuMPs, evidencing that the process of incorporation of the particles does not generate any conversion in the type of cellulose. T1 and T3 microparticle diffractograms presents three mean peaks at 2θ value of 43.29°, 50.35° and 74.04° (black asterisk) corresponding to the planes (111), (200) and (220) of *fcc* structure of metallic copper (JCPDS 85-1326) (Salavati-Niasari and Davar 2009). Additionally, seven peaks of less intensity (red asterisk) appears at 2θ value of 29.64°, 36.61°, 42.56°, 52.61°, 61.8°, 73.7° and 77.7° corresponding to Miller index (110), (111), (200), (211), (220), (311) and (222), respectively. All the peaks coincide with the reflections of standard cubic cuprite structure (JCPDS 78-2076) (Salavati-Niasari and Davar 2009). Other copper phases (cubic CuO) were not found in the diffractogram. The differences in the intensities of the two copper phases suggest that the microparticles are preferably metallic and a smaller amount corresponds to cuprous oxide (possibly associated with a slight surface oxidation).

The diffractograms of the papers with the CuMPs show a decrease in the intensity of the copper peaks

and therefore the planes associated with cuprous oxide disappear, possibly due to the lower content of microparticles against the amount of cellulose fibres. The results demonstrate that the preparation of the paper sheets with CuMPs maintain the metallic properties of the particles even after being immersed in water without ruling out any reduction of the Cu_2O due to the complete elimination of the planes of the cuprite phase in the diffractogram.

Moreover, atomic absorption spectroscopy (AAS) was used to determine the copper content embedded in the paper sheet, the results of which are shown in Table 4. A higher amount of incorporated copper was shown to result in a higher amount of embedded copper, in agreement with the UV–Vis spectroscopy results, where a direct proportionality between the CuMP concentration and the amplitude and area indices was observed. The percentages of embedded copper show, independent of the particle type and amount of copper incorporated, between 24 and 39% of copper was adsorbed onto the paper. This copper occupies an area between 1.812 and 2.530% of the total surface of the sheet, as determined from the results shown in Table 3.

After characterising the dispersion, distribution, and concentration of CuMPs incorporated into the paper sheets, we investigated the interaction between cellulose fibres and CuMPs by performing FTIR analyses. Figure 12 shows the spectra of papers made with different concentrations of T1 CuMPs and the control paper. Characteristic cellulose peaks associated with the O–H, C–H bonds at 3320 and 2910 cm^{-1}, respectively, were observed, as was a C–O–C-associated peak from 950 to 1200 cm^{-1} (Li et al. 2017). FTIR spectra for CuMP-paper were similar to that obtained for the paper without Cu, showing that CuMPs were adsorbed onto the cellulose fibre network through physical adsorption due to the chemical structure of cellulose remaining intact (Nakbanpote et al. 2007; He et al. 2018; Muthulakshmi et al. 2019) New peaks associated with copper interaction were not observed (Zhang et al. 2013; Goswami and Das 2018). Additionally, the presence of copper produced different spectral changes in the intensity of the peaks (Lázaro Martínez et al. 2008). This phenomenon can be attributed to an increase in

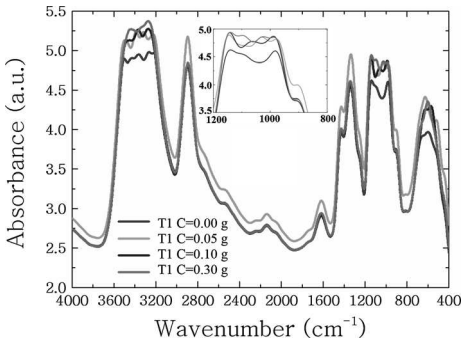

Fig. 12 FTIR spectra of papers with T1 copper particles at concentrations of 0.00, 0.05, 0.10, and 0.30 g

Table 4 Sample number and amount of incorporated and embedded copper (average of three measurements)

Sample No.	Particle type	Copper Incorporated (g)	Copper Embedded (g)	SD	Copper Embedded (%)
1	–	0.00	0	–	0
2	T1	0.05	0.021	0.003	34
3	T1	0.10	0.041	0.004	36
4	T1	0.30	0.104	0.010	39
5	T2	0.05	0.013	0.001	29
6	T2	0.10	0.041	0.004	35
7	T2	0.30	0.100	0.002	33
8	T3	0.05	0.012	0.001	24
9	T3	0.10	0.034	0.003	30
10	T3	0.30	0.089	0.010	31
11	T4	0.05	0.021	0.003	32
12	T4	0.10	0.028	0.003	32
13	T4	0.30	0.090	0.002	31

the intensity of the peaks. This could be attributed to the greater absorbance of the CuMP or to some kind of coordination of Cu with cellulose. Therefore, an additional interaction to adsorption can't be ruled out.

To determine whether the incorporation of CuMP modifies the structural, optical, and strength properties of the paper, a series of tests were performed according to paper industry standards. The results of physical and mechanical tests of the paper samples with CuMPs at different concentrations compared with those obtained for sample 1 of white paper without metal are shown in Fig. 13.

Figure 13 shows the effects of CuMPs on the structural properties of the paper, such as grammage, thickness, specific volume, and Gurley porosity. As the amount of copper increases, an increase in the weight, thickness, and specific volume of the sheet of paper was observed that was independent of the CuMP type. It is possible that the presence of copper particles prevents fibre aggregation. Gurley porosity values lower than the 2.8 s 100^{-1} cm^{-3} value of white paper were observed, with more significant decreases observed for papers made with the T1 and T2 copper particles than those made with the laminar T3 and T4 particles. The decrease in porosity was closely related to the increase in paper agglomeration, leading to an increase in the time needed to pass a certain volume of air through the sheet. With the T3 and T4 copper particles, incorporating laminar particles contributes to greater paper agglomeration due to their shape facilitating interactions parallel to the surface of the sheet, resulting in specific volume and Gurley porosity values that were closer to those of sample 1 without copper. Similar results have been obtained using 2% chitosan-coated paper, where lower Gurley porosity values were obtained after increasing air resistance readings by approximately 46% (Ashori et al. 2005).

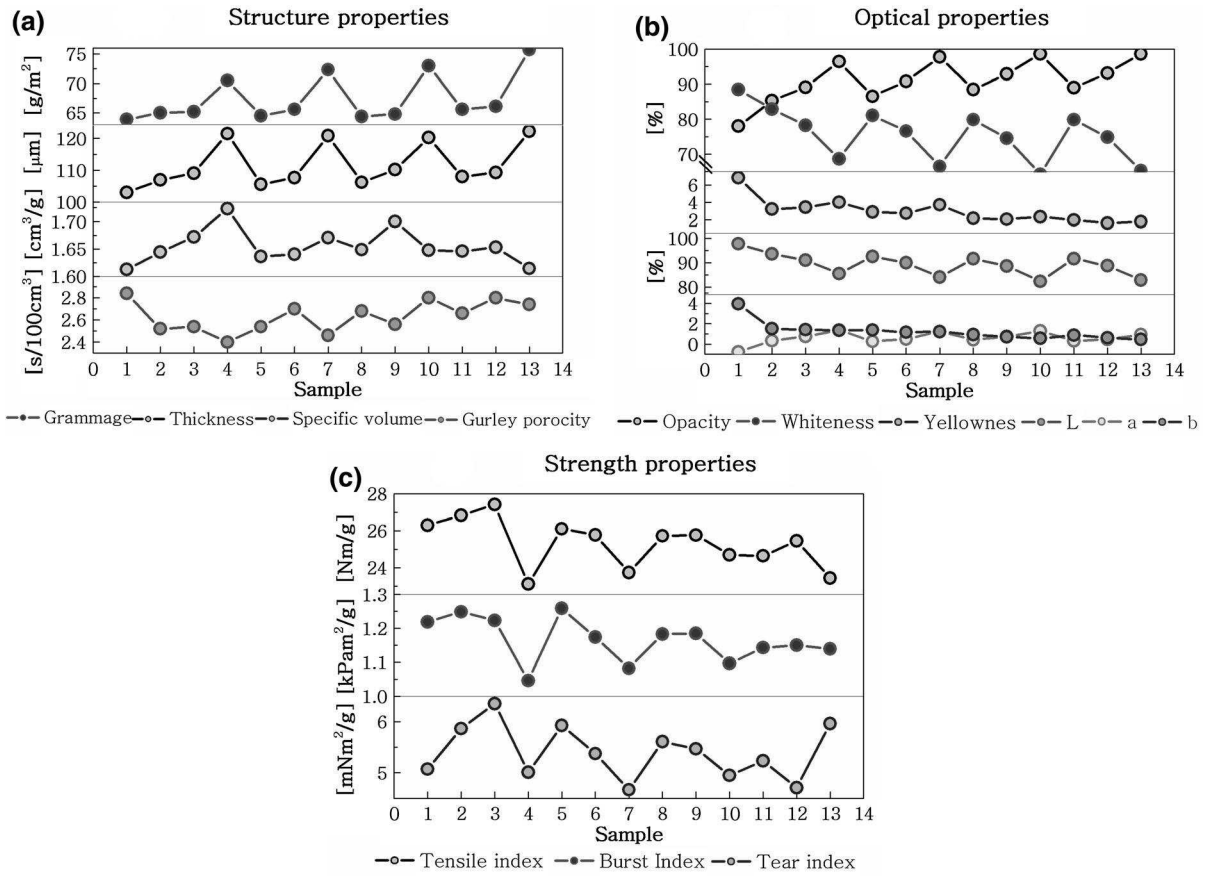

Fig. 13 Graphs of the structural **a**, **b** optical and **c** mechanical resistance properties of the different CuMP-containing papers and control samples without copper particles

Figure 13b shows the effect of the CuMPs on the paper optical properties, including opacity, whiteness, and the parameters L*, a* and b* defined by CIELAB, where L* corresponds to lightness, a* to colour from green (−) to red (+), and b* to colour from blue (−) to yellow (+) (Holik 2006). An increase in opacity and decrease in whiteness of paper occurred as the amount of copper increased, independent of the particle type, together with a decrease in the parameter L*, an increase in a*, and a decrease in b*. These changes were more evident after incorporating T3 and T4 particles, possibly because their laminar structure modifies the surface to a greater extent, having a greater effect on the optical properties. Changes in the colour of the paper are closely related to the colour of copper particles, affecting the staining they cause when incorporated into the paper fibres. This effect is demonstrated in Fig. 6, where the paper became browner as the copper concentration increased, with more intense hues observed by incorporating T3 and T4 copper particles.

The tensile strength, bursting strength, and tearing resistance indices relate to the strength properties of paper sheets, the values for which are shown in Fig. 13c. The higher the concentration of T1 and T2 copper particles, the more the values of these parameters increased compared with the control, reaching a maximum at 0.10 g of CuMPs, after which an abrupt decrease at 0.30 g of copper was observed. However, the sheets made with T3 and T4 particles did not show this tendency, with values lower or equal to the tensile strength and bursting strength indices of the control sample. The reason for this result may be that these paper sheets had lower specific volumes, were more compact, and were less pliable due to the stiffness of the copper particles with this morphology. Thus, when T1 and T2 particles are incorporated in high concentrations (0.30 g), the same effect of decreasing values for these indices were obtained.

Antimicrobial analysis

Finally, the CuMP concentration in the paper was correlated with its efficacy as an antimicrobial agent according to ISO 20645:2004, against strains of *S. aureus* and *K. pneumoniae*, two pathogens of clinical interest, to study whether they had different activities against Gram (+) and Gram (−) bacteria, the Table 5 shows the results of Fig. S5, interpreted according to ISO 20645:2004, on the inhibition of bacterial growth and the evaluation of the antibacterial effects. The papers with less than 0.30 g did not show an inhibition zone for either of the two strains, exhibiting a lack of antibacterial activity. Sample 12 in the test with *S. aureus* was the only one reaching the category of moderate, since the apparent size of the colonies decreased by half, as can be observed in the micrographs bacterial colonies in the samples stained with Coomassie blue R-250 (Table S6). Samples with 0.30 g of copper incorporated had a greater antibacterial effect against *S. aureus* than *K. pneumoniae*, since although an inhibition zone was present in the area of *K. pneumoniae* contact with the paper, the growth density was greater than that observed for *S. aureus*. This slight difference may occur because Gram (−) bacteria have a double membrane, possibly making them less susceptible to penetrating metal ions. This result is consistent with previous findings, where a difference in copper toxicity against Gram (+) bacteria compared to that observed for Gram (−) bacteria was observed (Azam et al. 2012).

The results show that the CuMPs have antimicrobial activity towards both bacterial strains assayed, independent of the shape of the CuMP incorporated into the paper, with the copper concentration being the determining factor for antimicrobial activity.

Since paper sheets obtained from incorporating 0.30 g of CuMPs (Samples No. 4, 7, 10, and 13) showed antimicrobial activity against *E. coli* and *K. pneumoniae*, four additional strains were assayed according to ISO 20645 and ISO 20743. All strains were selected for being pathogens of clinical interest, being *S. aureus* and *E. coli*, *K. pneumoniae* strains representative bacteria of Gram-positive and Gram-negative, respectively. *A. niger* fungi (present in hospital environments where spore propagation is favored through the use of air conditioning) was selected because of its ability to handle copper homeostatically. In contrast, *C. albicans* (an invasive fungus that affects immunosuppressed patients in hospitals) was selected for being representative of a pathogen without the ability to handle copper homeostatically.

Table 6 shows the results of the antimicrobial activity evaluations against strains of *S. aureus*, *E. coli*, *A. niger*, *C. albicans*, *and Penicillium* sp., performed according to ISO 20645 and ISO 20743. The results from ISO 20743 revealed that the CuMP-

Table 5 Effects of different particle types and copper contents in the paper sheets on the inhibition of bacterial growth and evaluation of the antibacterial effects

Sample No.	Bacteria	Inhibition zone (mm)	Bacterial growth[a]	Antibacterial effect[b]
2	*S. aureus*	0	D	I
	K. pneumoniae	0	D	I
3	*S. aureus*	0	D	I
	K. pneumoniae	0	D	I
4	*S. aureus*	2	N	G
	K. pneumoniae	2.75	N	G
5	*S. aureus*	0	D	I
	K. pneumoniae	0	D	I
6	*S. aureus*	0	D	I
	K. pneumoniae	0	D	I
7	*S. aureus*	4.25	N	G
	K. pneumoniae	3.4	N	G
8	*S. aureus*	0	D	I
	K. pneumoniae	0	D	I
9	*S. aureus*	0	D	I
	K. pneumoniae	0	D	I
10	*S. aureus*	4.1	N	G
	K. pneumoniae	3.1	N	G
11	*S. aureus*	0	D	I
	K. pneumoniae	0	D	I
12	*S. aureus*	0	M	I
	K. pneumoniae	0	D	I
13	*S. aureus*	4.6	N	G
	K. pneumoniae	4.55	N	G

[a]Growth: *N* none, *S* slight, *M* moderate, *D* dense

[b]Effect: *I* insufficient, *L* limit of efficacy, *G* good

paper exhibited strong antibacterial activity against *S. aureus*, (consistent with previous tests) and *E. coli*, a Gram (−) bacterium. Strong antifungal activity was also observed against *C. albicans*, and sufficient activity was observed against *A. niger* and *Penicillium* sp. In contrast, according to ISO 20645, the observed effect reached the category of good against *S. aureus* and *E. coli*, the limit of efficacy against *A. niger*, and had an insufficient effect against *C. albicans* and *Penicillium* sp. These results revealed that ISO 20743 was more sensitive than ISO 20645 for determining the antimicrobial effects of the various papers. In the first method, the direct contact between the microorganism and the sample occurred in suspension, promoting the release and diffusion of copper ions from the paper into the aqueous phase (see additional diffusion experiment in S7). These ions came into contact with the outer membrane of the pathogen, promoting microbial death on contact without having to diffuse through the agar matrix as occurs in disc diffusion tests, showing that their release and diffusion depends on the medium (Adeleye et al. 2014).

No significant differences were observed with respect to the effects of the various papers on Gram (+) and Gram (−) bacteria. However, differences in their antifungal effects were observed, since *C. albicans* was much more sensitive, which is in agreement with previous observations in which this greater sensitivity of *C. albicans* was attributed to a lack of ATPase transporters. These proteins are involved in regulating intracellular copper levels, resulting in its accumulation (Quaranta et al. 2011). Notably, in contrast to the results reported by Weaver et al. (Weaver et al. 2010), in this study, CuMP-paper showed an effect against *A. niger*.

The effects of different incubation times (0, 0.5, 1, 2, and 3 h) were studied to determine the minimum time necessary for the paper sheet samples to exert their antimicrobial effects by evaluating mixed T1 and laminar T3 particles. Table 7 shows the results of these

Table 6 Evaluation of the antimicrobial activities of paper sheets containing copper microparticles, performed according to ISO 20645 and ISO 20743 (average of three measurements)

Sample No.	ISO	*S. aureus*		*E. coli*		*A. niger*		*C. albicans*		*Penicillium* sp.	
		H/A[b]	Effect[a]	H/A	Effect	H/A	Effect	H/A	Effect	H/A	Effect
4	20645	3.3 ± 0.06	G	2.5 ± 0.05	G	0	L	0	I	0	I
	20743	5.92 ± 0.04	St	7.06 ± 0.07	St	2.04 ± 0.05	S	4.65 ± 0.06	St	1.04 ± 0.04	S
7	20645	2.8 ± 0.05	G	3 ± 0.06	G	0	L	0	I	0	I
	20743	9.59 ± 0.08	St	6.63 ± 0.08	St	3.04 ± 0.04	St	3.81 ± 0.05	St	1.18 ± 0.04	S
10	20645	3 ± 0.08	G	2.8 ± 0.06	G	0	L	0	I	0	I
	20743	6.43 ± 0.07	St	–		2.88 ± 0.04	S	4.16 ± 0.05	St	1.56 ± 0.05	S
13	20645	4 ± 0.1	G	2.8 ± 0.05	G	0	L	0	I	0	I
	20743	5.13 ± 0.05	St	–		2.96 ± 0.04	S	3.49 ± 0.06	St	2.24 ± 0.04	S

[a]ISO 20645 effect: *I* insufficient, *L* limit of efficacy, *G* good. ISO 20743: *S* significant, *St* strong

[b]ISO 20645 antimicrobial activity: H value (mm). ISO 20743: A value (activity)

assays, where for *E. coli* and *S. aureus*, antimicrobial activity was observed early on (0.5 h), both in samples 4 and 10. However, against *A. niger*, significant antifungal activity was only observed after 2 h for the sample with mixed CuMPs (Sample No. 4) and after 0.5 h for the laminar CuMP-paper (Sample No. 10). These results are probably due to greater copper exposure in the paper sample with laminar copper microparticles due to the more superficial orientation with cellulose fibres and the copper homeostasis characteristics of *A. niger* (Weaver et al. 2010).

The results showed the varied efficacy of copper in both formats towards *S. aureus* at different exposure times, which may be related to the oxidative state of copper and its solubility, both factors closely associated with antimicrobial activity (Vincent et al. 2016; Hans et al. 2016), or to a copper resistance mechanism of the assayed bacteria. However, such resistance would not last long (Liu and Zhang 2016), as membrane damage would not be the only mechanism to initiate death on contact (Warmes and Keevil 2016).

Conclusions

The results of this study have aided in the evaluation of different methods for incorporating mixed or laminar copper microparticles during papermaking, correlating their concentration and shape in cellulose fibres with antimicrobial properties.

The paper sheets produced using two methods to incorporate CuMPs during the different paper-making steps were characterised by optical microscopy and UV–Vis spectroscopy. The results showed that incorporating CuMPs at an early manufacturing stage produces sheets with a homogeneous distribution of CuMPs. This result was confirmed by optical micrographs and by determining the values of two indices (the intensity at 450 nm and the area under the spectrum) obtained from UV–Vis absorption spectra at different areas of the papers. These results allowed us to correlate these indices with the CuMP concentration in the paper and predict future results associated with the use of other copper concentrations. The method of incorporating CuMPs at an early stage was selected for further studies because of the good distribution of CuMPs achieved among the fibres. These results occurred due to the copper particles being in contact with the cellulose fibres from the first

Table 7 Evaluation of the antimicrobial activities of paper sheets containing copper microparticles at different times of exposure to the assayed microorganisms, performed according to ISO 20743 (average of three measurements)

Sample No.	Time (h)	*S. aureus*		*E. coli*		*A. niger*	
		A	Efficacy	A	Efficacy	A	A
4	0.5	3.56 ± 0.04	St	3.30 ± 0.04	4	0.5	3.56 ± 0.04
	1	2.22 ± 0.04	S	3.77 ± 0.04	St	1	2.22 ± 0.04
	2	2.63 ± 0.05	S	4.52 ± 0.05	St	2	2.63 ± 0.05
	3	4.89 ± 0.07	St	3.46 ± 0.05	St	3	4.89 ± 0.07
10	0.5	3.19 ± 0.05	St	1.54 ± 0.06	10	0.5	3.19 ± 0.05
	1	1.23 ± 0.06	S	3.64 ± 0.07	St	1	1.23 ± 0.06
	2	0.30 ± 0.05	S	4.35 ± 0.06	St	2	0.30 ± 0.05
	3	4.60 ± 0.04	St	2.45 ± 0.05	S	3	4.60 ± 0.04

ISO 20743 Activity: *N* none, *Sl* slight, *S* significant, *St* strong

step of papermaking, whereas the incorporation of copper during the sheet-forming stage produced CuMP-paper with poor dispersion and uneven distribution among the cellulose fibres.

Papers containing different concentrations of CuMPs were characterised by a series of bright-field, dark-field, and fluorescence optical micrographs as well as by SEM micrographs. The results of these analyses allowed the cellulose fibres and the reflection of copper particles in the fibre vessels to be observed in detail such that size distribution histograms of the copper particles could be generated, as well as for 3D visualisations of the particles incorporated into the paper. The findings confirmed the direct proportionality between the concentration of incorporated and embedded copper. The X-ray analysis showed that there is no conversion in the type of cellulose as a result of from the incorporation of CuMPs. Additionally, the presence of the three Bragg's reflections with greater intensity confirm that the microparticles mainly maintained a metallic state. Atomic absorption analysis showed that between 24 and 39% of the CuMPs were embedded in the paper fibres, independent of particle type, and that the primary incorporation route was physisorption due the FTIR spectra not showing the presence of chemical bonds.

The results of physical and mechanical tests showed a direct correlation between the copper concentration and the structural, optical, and strength properties of the papers made with CuMPs compared with the white paper. The difference was most evident when incorporating laminar CuMPs, which resulted in their surface deposition on cellulose fibres. Importantly, the paper maintained standards according to industry requirements for use in various applications.

Finally, antimicrobial analyses of papers with different CuMP content against *S. aureus* and *K. pneumoniae* strains, performed according to ISO 20645, showed that the papers made with 0.30 g of CuMPs exhibited antimicrobial activity, independent of particle shape, with similar activities observed towards Gram (+) and Gram (−) bacteria. Notably, because the antimicrobial activity of CuMP-paper probably begins at amounts less than 0.30 g and greater than 0.10 g of CuMPs, optimising the copper concentration is still necessary. Antimicrobial analyses using ISO 20645 and ISO 20743 for samples with 0.30 g of CuMPs against the Gram (+) and Gram (−) bacteria *S. aureus* and *E. coli*, as well as fungi such as *C. albicans*, *A. niger*, and *Penicillium* sp. revealed that the ISO 20743 quantitative standard is more sensitive than ISO 20645 for determining the antifungal effects of CuMP paper. The results of the evaluations of the antimicrobial activity of CuMP paper at different times of exposure towards the microorganisms showed that the different antimicrobial activities was related to the shape of the CuMPs incorporated into the paper. The laminar CuMPs exerted a sufficient effect compared with the null or slight effect of the mixed CuMPs against *A. niger*, which agreed with the results of previous characterisations due to the greater area of exposed copper.

This study demonstrated that the previously unreported use of CuMPs in paper provides a biocidal

effect, which was slightly better when laminar CuMPs were used compared with mixed particles. Compared with smaller copper particles, the use of CuMPs could reduce the potential for genotoxicity.

These results suggest that CuMP-paper is a valuable biocidal technology for the industrial application of paper with resistance to degradation by microorganisms, including in food packaging, filters, sensors, and medical supplies.

Acknowledgments The authors would like to thank Eckart Eitner, Raúl González, Cristian Segura, and Felipe Torres of the CMPC; Nancy Pérez and Rodrigo del Canto of the ICono UDD technological development office; and Benjamín Erranz and INTA for antimicrobial analysis services. Additional thanks to the funding granted by a UDD internal research competition and to an UDD institutional contribution. R. Lavín acknowledges financial support in Chile from the Basic Financing for Scientific and Technological Centres of Excellence under Grant AFB180001.

Funding Funding was provided by Universidad del Desarrollo (Grant No. 23400091).

Compliance with ethical standards

Conflict of interest The authors declare that they have no conflict of interest.

Appendix

Antibacterial activity, according to ISO 20645, was calculated using the formula:

$$H = \frac{D - d}{2} \quad (1)$$

where H corresponds to the inhibition zone; D: total sample diameter and inhibition zone; and d: sample diameter, all expressed in mm.

Antibacterial effect is defined according to the criteria in Table 8 (ISO 20645).

Antibacterial activity, according to ISO 20743, was calculated with the formula:

$$A = \left(I_g C_t - I_g C_o\right) - \left(I_g T_t - I_g T_o\right) = F - G \quad (2)$$

where A corresponds to the value of the antibacterial activity; F: count of viable bacteria in the control sample ($F = I_g C_t - I_g C_O$); G: count of viable bacteria in the experimental samples ($G = I_g T_t - I_g C_T$); I_gT_t: average common logarithm for the number of bacteria obtained from a triplicate of three experimental samples after 18–24 h of incubation; and I_gT_o: average common logarithm for the number of bacteria obtained from a triplicate of three experimental samples immediately after inoculation.

The value obtained from the formula above was compared with that obtained for controls using interpretation ranges (Table 9) as proposed by the Hohenstein Research Institute (2008).

Table 9 Interpretation ranges of antimicrobial activity proposed by the Hohenstein Research Institute

Antimicrobial activity	Specific efficacy
None	< 0.5
Slight	$0.5 < 1$
Significant	$1 < 3$
Strong	≥ 3

Table 8 Antibacterial effect according to ISO 20645 criteria for antibacterial treatment

Inhibition zone (mm) mean value	Growth	Description	Assessment
> 1	None	Inhibition zone exceeding 1 mm, no growth	
1–0	None	Inhibition zone up to 1 mm, no growth	Good effect
0	None	No inhibition zone, no growth	
0	Slight	No inhibition zone, only some restricted colonies, growth nearly totally suppressed	Limit of efficacy
0	Moderate	No inhibition zone, compared to the control growth reduced to half	Insufficient effect
0	Heavy	No inhibition zone, compared to the control no growth reduction or only slightly reduced growth	

References

Adeleye AS, Conway JR, Perez T et al (2014) Influence of extracellular polymeric substances on the long-term fate, dissolution, and speciation of copper-based nanoparticles. Environ Sci Technol 48:12561–12568. https://doi.org/10.1021/es5033426

Amini E, Azadfallah M, Layeghi M, Talaei-Hassanloui R (2016) Silver-nanoparticle-impregnated cellulose nanofiber coating for packaging paper. Cellulose 23:557–570. https://doi.org/10.1007/s10570-015-0846-1

Ashori A, Raverty WD, Harun J (2005) Effect of chitosan addition on the surface properties of kenaf (*Hibiscus cannabinus*) paper. Fibers Polym 6:174–179. https://doi.org/10.1007/BF02875611

Azam A, Ahmed O et al (2012) Antimicrobial activity of metal oxide nanoparticles against Gram-positive and Gram-negative bacteria: a comparative study. Int J Nanomed 7:6003–6009. https://doi.org/10.2147/IJN.S35347

Cano AP, Gillado AV, Montecillo AD, Herrera MU (2018) Copper sulfate-embedded and copper oxide-embedded filter paper and their antimicrobial properties. Mater Chem Phys 207:147–153. https://doi.org/10.1016/j.matchemphys.2017.12.049

Chardon WJ, Menon RG, Chien SH (1996) Iron oxide impregnated filter paper (Pi test): a review of its development and methodological research. Nutr Cycl Agroecosyst 46:41–51. https://doi.org/10.1007/BF00210223

Chen PC, Li YC, Ma JY et al (2016) Size-tunable copper nanocluster aggregates and their application in hydrogen sulfide sensing on paper-based devices. Sci Rep 6:1–9. https://doi.org/10.1038/srep24882

Dankovich TA, Gray DG (2011) Bactericidal paper impregnated with silver nanoparticles for point-of-use water treatment. Environ Sci Technol 45:1992–1998. https://doi.org/10.1021/es103302t

Dankovich TA, Levine JS, Potgieter N et al (2016) Inactivation of bacteria from contaminated streams in Limpopo, South Africa by silver- or copper-nanoparticle paper filters. Environ Sci Water Res Technol 2:85–96. https://doi.org/10.1039/c5ew00188a

Dankovich TA, Smith JA (2014) Incorporation of copper nanoparticles into paper for point-of-use water purification. Water Res 63:245–251. https://doi.org/10.1016/j.watres.2014.06.022

Dector A, Galindo-de-la-Rosa J, Amaya-Cruz DM et al (2017) Towards autonomous lateral flow assays: paper-based microfluidic fuel cell inside an HIV-test using a blood sample as fuel. Int J Hydrog Energy 42:27979–27986. https://doi.org/10.1016/j.ijhydene.2017.07.079

Emam HE, Manian AP, Široká B et al (2014) Copper(I)oxide surface modified cellulose fibers—synthesis, characterization and antimicrobial properties. Surf Coat Technol 254:344–351. https://doi.org/10.1016/j.surfcoat.2014.06.036

Esquivel JP, Del Campo FJ, Gómez De La Fuente JL et al (2014) Microfluidic fuel cells on paper: meeting the power needs of next generation lateral flow devices. Energy Environ Sci 7:1744–1749. https://doi.org/10.1039/c3ee44044c

Esquivel JP, Buser JR, Lim CW et al (2017) Single-use paper-based hydrogen fuel cells for point-of-care diagnostic applications. J Power Sources 342:442–451. https://doi.org/10.1016/j.jpowsour.2016.12.085

Fawcett RG, Collis-George N (1967) A filter-paper method for determining the moisture characteristics of soil. Aust J Exp Agric 7:162–167. https://doi.org/10.1071/EA9670162

Ghorbani HR (2014) Biological coating of paper using silver nanoparticles. IET Nanobiotechnol 8:263–266. https://doi.org/10.1049/iet-nbt.2013.0039

Ghorbani HR (2017) Preparation of chitosan-copper nanoparticles coated Kraft paper, characterization and its antimicrobial activity. J Nanoanal 4:320–323. https://doi.org/10.22034/JNA.2018.552110.1049

Gong J, Li J, Xu J et al (2017) Research on cellulose nanocrystals produced from cellulose sources with various polymorphs. RSC Adv 7:33486–33493. https://doi.org/10.1039/c7ra06222b

Goswami M, Das AM (2018) Synthesis of cellulose impregnated copper nanoparticles as an efficient heterogeneous catalyst for C–N coupling reactions under mild conditions. Carbohyd Polym 195:189–198. https://doi.org/10.1016/j.carbpol.2018.04.033

Hans M, Mathews S, Mücklich F, Solioz M (2016) Physicochemical properties of copper important for its antibacterial activity and development of a unified model. Biointerphases 11:018902. https://doi.org/10.1116/1.4935853

He W, Huang X, Zheng Y et al (2018) In situ synthesis of bacterial cellulose/copper nanoparticles composite membranes with long-term antibacterial property. J Biomater Sci Polym Ed 29:2137–2153. https://doi.org/10.1080/09205063.2018.1528518

Holik H (2006) Handbook of paper and board, Sixta. Wiley, Weinheim

Huang X, Hu N, Wang X et al (2017) Copper sulfide nanoparticle/cellulose composite paper: room-temperature green fabrication for NIR laser-inducible ablation of pathogenic microorganisms. ACS Sustain Chem Eng 5:2648–2655. https://doi.org/10.1021/acssuschemeng.6b03003

Imani R, Talaiepour M, Dutta J et al (2011) Production of antibacterial filter paper from wood cellulose. BioResources 6:891–900. https://doi.org/10.15376/biores.6.1.891-900

Jain S, Bhanjana G, Heydarifard S et al (2018) Enhanced antibacterial profile of nanoparticle impregnated cellulose foam filter paper for drinking water filtration. Carbohyd Polym 202:219–226. https://doi.org/10.1016/j.carbpol.2018.08.130

Jia B, Mei Y, Cheng L et al (2012) Preparation of copper nanoparticles coated cellulose films with antibacterial properties through one-step reduction. ACS Appl Mater Interfaces 4:2897–2902. https://doi.org/10.1021/am3007609

Jokerst JC, Emory JM, Henry CS (2012) Advances in microfluidics for environmental analysis. Analyst 137:24–34. https://doi.org/10.1039/c1an15368d

Kaweeteerawat C, Chang CH, Roy KR et al (2015) Cu nanoparticles have different impacts in *Escherichia coli* and *Lactobacillus brevis* than their microsized and ionic

analogues. ACS Nano 9:7215–7225. https://doi.org/10.1021/acsnano.5b02021

Kim J, Lee H, Kim HS (2010) Beam vibration control using cellulosebased electro-active paper sensor. Int J Precis Eng Manuf 11:823–827. https://doi.org/10.1007/s12541-010-0099-8

Koziróg A, Brycki B, Olejnik K et al (2019) Cellulose products modified with monomeric and gemini surfactants: antimicrobial aspects. Cellulose 26:5559–5570. https://doi.org/10.1007/s10570-019-02475-0

Kunkel HG (1951) Electrophoresis of proteins on filter paper. J Gen Physiol 35:89–118. https://doi.org/10.1085/jgp.35.1.89

Lázaro Martínez JM, Chattah AK, Monti GA et al (2008) New copper(II) complexes of polyampholyte and polyelectrolyte polymers: solid-state NMR, FTIR, XRPD and thermal analyses. Polymer 49:5482–5489. https://doi.org/10.1016/j.polymer.2008.10.011

Li H, Cui R, Peng L et al (2017) Preparation of antibacterial cellulose paper using layer-by-layer assembly for cooked beef preservation at ambient temperature. Polymers 10:15. https://doi.org/10.3390/polym10010015

Liang J, Wang Y, Liu B (2012) Paper-based fluoroimmunoassay for rapid and sensitive detection of antigen. RSC Adv 2:3878–3884. https://doi.org/10.1039/c2ra20156a

Liu S, Zhang XX (2016) Small colony variants are more susceptible to copper-mediated contact killing for *Pseudomonas aeruginosa* and *Staphylococcus aureus*. J Med Microbiol 65:1143–1151. https://doi.org/10.1099/jmm.0.000348

Łojewska J, Missori M, Lubańska A et al (2007) Carbonyl groups development on degraded cellulose. Correlation between spectroscopic and chemical results. Appl Phys A Mater Sci Process 89:883–887. https://doi.org/10.1007/s00339-007-4220-5

Mahadeva SK, Yun S, Kim J (2011) Flexible humidity and temperature sensor based on cellulose-polypyrrole nanocomposite. Sens Actuators A Phys 165:194–199. https://doi.org/10.1016/j.sna.2010.10.018

Martins NCT, Freire CSR, Neto CP et al (2013) Antibacterial paper based on composite coatings of nanofibrillated cellulose and ZnO. Colloids Surf A Physiochem Eng 417:111–119. https://doi.org/10.1016/j.colsurfa.2012.10.042

Maurer HW (2009) Starch in the paper industry, 3rd edn. Elsevier Inc, Amsterdam

Mei JV, Alexander JR, Adam BW, Hannon H (2001) Use of filter paper for the collection and analysis of human whole blood specimens. J Nutr 13:1631–1636. https://doi.org/10.1093/jn/131.5.1631S

Mousavi Ehteshami SM, Asadnia M, Tan SN, Chan SH (2016) Paper-based membraneless hydrogen peroxide fuel cell prepared by micro-fabrication. J Power Sources 301:392–395. https://doi.org/10.1016/j.jpowsour.2015.10.038

Muthulakshmi L, Varada Rajalu A, Kaliaraj GS et al (2019) Preparation of cellulose/copper nanoparticles bionanocomposite films using a bioflocculant polymer as reducing agent for antibacterial and anticorrosion applications. Compos B Eng 175:107177. https://doi.org/10.1016/j.compositesb.2019.107177

Nakbanpote W, Goodman BA, Thiravetyan P (2007) Copper adsorption on rice husk derived materials studied by EPR and FTIR. Colloids Surf A Physiochem Eng 304:7–13. https://doi.org/10.1016/j.colsurfa.2007.04.013

Nechita P, Bobu E, Parfene G et al (2015) Antimicrobial coatings based on chitosan derivatives and quaternary ammonium salts for packaging paper applications. Cellul Chem Technol 49:625–632

Nery EW, Kubota LT (2013) Sensing approaches on paper-based devices: a review. Anal Bioanal Chem 405:7573–7595. https://doi.org/10.1007/s00216-013-6911-4

Ngo YH, Li D, Simon GP, Garnier G (2011) Paper surfaces functionalized by nanoparticles. Adv Coll Interface Sci 163:23–38. https://doi.org/10.1016/j.cis.2011.01.004

Pang B, Yan J, Yao L et al (2016) Preparation and characterization of antibacterial paper coated with sodium lignosulfonate stabilized ZnO nanoparticles. RSC Adv 6:9753–9759. https://doi.org/10.1039/c5ra21434c

Quaranta D, Krans T, Santo CE et al (2011) Mechanisms of contact-mediated killing of yeast cells on dry metallic copper surfaces. Appl Environ Microbiol 77:416–426. https://doi.org/10.1128/AEM.01704-10

Salavati-Niasari M, Davar F (2009) Synthesis of copper and copper(I) oxide nanoparticles by thermal decomposition of a new precursor. Mater Lett 63:441–443. https://doi.org/10.1016/j.matlet.2008.11.023

Sequeira S, Cabrita EJ, Macedo MF (2012) Antifungals on paper conservation: an overview. Int Biodeterior Biodegrad 74:67–86. https://doi.org/10.1016/j.ibiod.2012.07.011

Shankar S, Rhim J (2018) Antimicrobial wrapping paper coated with a ternary blend of carbohydrates (alginate, carboxymethyl cellulose, carrageenan) and grapefruit seed extract. Carbohyd Polym 196:92–101. https://doi.org/10.1016/j.carbpol.2018.04.128

Silva N, Ramírez S, Díaz I et al (2019) Easy, quick, and reproducible sonochemical synthesis of CuO nanoparticles. Materials 12:804–817. https://doi.org/10.3390/ma12050804

Szekeres GP, Nemeth Z, Schrantz K et al (2018) Copper-coated cellulose-based water filters for virus retention. ACS Omega 3:446–454. https://doi.org/10.1021/acsomega.7b01496

Tamayo L, Azócar M, Kogan M et al (2016) Copper-polymer nanocomposites: an excellent and cost-effective biocide for use on antibacterial surfaces. Mater Sci Eng C 69:1391–1409. https://doi.org/10.1016/j.msec.2016.08.041

Tsai TT, Huang TH, Chang CJ et al (2017) Antibacterial cellulose paper made with silver-coated gold nanoparticles. Sci Rep 7:1–10. https://doi.org/10.1038/s41598-017-03357-w

Vartiainen J, Motion R, Kulonen H et al (2004) Chitosan-coated paper: effects of nisin and different acids on the antimicrobial activity. J Appl Polym Sci 94:986–993. https://doi.org/10.1002/app.20701

Vincent M, Hartemann P, Engels-Deutsch M (2016) Antimicrobial applications of copper. Int J Hyg Environ Health 219:585–591. https://doi.org/10.1016/j.ijheh.2016.06.003

Wang J, Liu W, Li H et al (2013) Preparation of cellulose fiber-TiO_2 nanobelt-silver nanoparticle hierarchically structured

hybrid paper and its photocatalytic and antibacterial properties. Chem Eng J 228:272–280. https://doi.org/10.1016/j.cej.2013.04.098

Wang S, Ge L, Song X et al (2012) Simple and covalent fabrication of a paper device and its application in sensitive chemiluminescence immunoassay. Analyst 137:3821–3827. https://doi.org/10.1039/c2an35266d

Warmes SL, Keevil W (2016) Death and genome destruction of methicillin-resistant and methicillin-sensitive strains of *Staphylococcus aureus* on wet or dry copper alloy surfaces does not involve Fenton chemistry. Appl Environ Microbiol 82:2132–2136. https://doi.org/10.1128/aem.03861-15

Weaver L, Michels HT, Keevil CW (2010) Potential for preventing spread of fungi in air-conditioning systems constructed using copper instead of aluminium. Lett Appl Microbiol 50:18–23. https://doi.org/10.1111/j.1472-765X.2009.02753.x

Xu Y, Li S, Yue X, Lu W (2018) Review of Silver nanoparticles (AgNPs)-cellulose antibacterial composites. BioResources 13:2150–2170. https://doi.org/10.15376/biores.13.1.Xu

Zhai L, Park J, Lee JY et al (2018) Synthesis, characterization, and antibacterial property of eco-friendly Ag/cellulose nanocomposite film. Int J Polym Mater Polym Biomater 67:420–426. https://doi.org/10.1080/00914037.2017.1342247

Zhang YX, Huang M, Li F, Wen ZQ (2013) Controlled synthesis of hierarchical CuO nanostructures for electrochemical capacitor electrodes. Int J Electrochem Sci 8:8645–8661